Published in final edited form as:

Biochim Biophys Acta. 2016 July ; 1863(7 Pt B): 1717–1727. doi:10.1016/j.bbamcr.2016.03.003.

High Throughput Physiological Screening of iPSC-Derived Cardiomyocytes for Drug Development

Juan Carlos del Álamo[1], **Derek Lemons**[2,3,5], **Ricardo Serrano**[1], **Alex Savchenko**[2,3,5], **Fabio Cerignoli**[4], **Rolf Bodmer**[3], and **Mark Mercola**[2,3,5,*]

[1]Department of Mechanical and Aerospace Engineering, University of California, San Diego, 9500 Gilman Drive MC 0411, La Jolla, CA 92093-0411

[2]Department of Bioengineering, University of California, San Diego, 9500 Gilman Drive MC 0412, La Jolla, CA 92093-0412

[3]Sanford-Burnham-Prebys Medical Discovery Institute, 10901 N. Torrey Pines Road, La Jolla, CA 92037

[4]ACEA Biosciences, Inc., 6779 Mesa Ridge Road, San Diego, CA 92121

[5]Stanford Cardiovascular Institute, 265 Campus Dr. Stanford, CA 94305-5454

Abstract

Cardiac drug discovery is hampered by the reliance on non-human animal and cellular models with inadequate throughput and physiological fidelity to accurately identify new targets and test novel therapeutic strategies. Similarly, adverse drug effects on the heart are challenging to model, contributing to costly failure of drugs during development and even after market launch. Human induced pluripotent stem cell derived cardiac tissue represents a potentially powerful means to model aspects of heart physiology relevant to disease and adverse drug effects, providing both the human context and throughput needed to improve the efficiency of drug development. Here we review emerging technologies for high throughput measurements of cardiomyocyte physiology, and comment on the promises and challenges of using iPSC-derived cardiomyocytes to model disease and introduce the human context into early stages of drug discovery.

Keywords

drug discovery; high content screening; cardiomyocyte; heart; physiology; automated microscopy; particle image velocimetry

*To whom correspondence should be addressed at ; Email: mmercola@stanford.edu

Introduction

Advances in the production of differentiated cells from induced pluripotent stem cells (iPSCs) make it possible to create models of cardiovascular disease with sufficient robustness for high throughput applications. Combined with pharmaceutical-style assay development and screening, and the availability of chemical and oligonucleotide libraries to probe protein and gene function, researchers now have the unprecedented opportunity to probe fundamental disease mechanisms in a comprehensive and unbiased way.

These new technologies create enormous potential for early stage drug discovery. The modern drug development paradigm commonly uses biochemical or reductionist cell culture models for initial drug screening, while animal models are used later as *in vivo* models. The human context is typically implemented relatively late in the discovery process after lead compounds have been identified. Similarly, target identification, although clearly motivated by human disease, typically proceeds from studies of disease mechanisms that focus on one or relatively few hypotheses rather than from large-scale unbiased testing, although the revolution in genomics is rapidly changing target identification. iPSC disease modeling combined with pharmaceutical company-style high throughput approaches enable compound screening as well as large-scale, unbiased screening for drug targets as well. Thus, iPSC disease modeling represents a paradigm shift that re-introduces the human context early in the discovery pipeline that is reminiscent of earlier days in drug development when drugs were discovered based on clinical experience.

For heart disease, physiological assays that measure cardiomyocyte function are particularly important to reveal drug effects and discover new therapeutic targets Physiological assays, such as patch clamp recording, were historically too low throughput to implement in large scale experiments, and, therefore, unsuitable for unbiased approaches to probe basic disease mechanisms or for initial drug screening. With the emergence of automated microscopy, along with fast and highly fluorescent voltage and calcium sensors, it has become possible to develop high content screening platforms and assays with the ability to measure kinetic parameters of cardiomyocyte function.

This review summarizes state-of-the-art technologies for high throughput measurements of cardiomyocyte physiology, and comments on the promises and shortcomings of iPSC-derived cardiomyocytes to advance research into fundamental disease mechanisms and introduce the human context into early stages of drug discovery. Although drug discovery and basic research to delineate disease mechanisms differ in the conceptual design of experiments and the technological approaches to execute them, our philosophy is that both will benefit from iPSC-cardiomyocyte models that recapitulate disease and have the throughput to enable large-scale chemical or functional genomics screening. Therefore, we focus on emerging technological advances that we hope will create high throughput and high fidelity models of human cardiovascular disease.

Producing iPSC-cardiomyocytes for disease modeling

The ability to easily induce pluripotent stem cells sparked a revolution in the thinking of development as a one-way timeline from egg to organism, and in theory enabled the production of every cell type in the body as long as we can develop culture conditions to direct differentiation appropriately. For cardiovascular lineages, the efficient production of cardiomyocytes, vascular endothelial cells, and smooth muscle cells is now feasible thanks to decades of research into basic embryology and developmental biology. Classical microdissection experiments, using amphibian embryos and juxtaposing candidate inducing tissues to the heart field prior to specification, suggested an inductive role for the endoderm that gives rise to pharynx [1–7] and additional signals located in future craniofacial mesoderm [7, 8]. Similar classical studies with cultured chick embryos also suggested that both embryonic (hypoblast) and definitive endoderm produce heart-inducing signals [9–11].

One class of particularly potent cardiomyogenic inducing molecules turned out to be Wnt antagonists. The secreted protein Dickkopf-1 and the secreted Frizzled domain protein Crescent-1 were the first identified [12, 13], as reviewed [14]. Subsequently, small molecule Wnt inhibitors were shown to substitute for Dkk1 in producing cardiomyocytes from pluripotent stem cells [15].

First generation protocols that optimized the embryological inducers for the production of cardiac tissues induced by Wnt inhibition, either DKK1 or small molecule inhibitors, from pluripotent stem cell cultures originally produced approximately 10–50% cardiomyocytes along with vascular endothelial cells, smooth muscle cells and fibroblasts, among other cell types [16]. Later refinements focused on individual cardiovascular lineages, with notable protocols for cardiomyocytes [17–19]. These second generation protocols turned out to be quite efficient and enabled reproducible cardiomyocyte production from numerous embryonic stem cell (ESC) and iPSC cell lines. Several questions relevant to the use of iPSC cardiomyocytes remain unanswered, including whether the ventricular cardiomyocytes produced are typical of the left or right ventricle, and the ideal factors that can direct the differentiation of particular subsets of cardiomycytes (e.g. atrial versus ventricular and nodal cardiomyocytes).

Despite these uncertainties, commercially produced hPSC-cardiomyocytes are now available from several vendors, charging approximately $1,000–2,000 per vial of about 1 million highly enriched (~90% purity) cardiomyocytes. In addition to answering the questions above, it is hoped that iPSC-cardiomyocytes will soon be produced in large quantities at considerably lower cost, and that the production from patient samples will become more widespread than today, partly as a result of commercialization of the reprogramming and directed differentiation processes.

Electrophysiological characterization of iPSC cardiomyocytes, produced by various protocols and cultured in simple, two dimensional monolayer cultures typically on stiff substrates such as cell culture dish plastic, reveals that they contain most of the cardiac ion currents present in adult cardiomyocytes but nonetheless are immature [20, 21]. Important distinctions between iPSC-cardiomyocytes and adult cardiomyocytes are that they are

deficient in I_{K1}, which is important for the normally low resting potential of mature cardiomyocytes and also presence of the $I_f Ca^{2+}$ current that that contributes to automaticity by causing a slow depolarization between beats that results in the cell's membrane potential rising to the threshold for Na^+ channel opening (−50 mV), summarized by Knollman [22] and Keung et al. [23] and Table 1. I_{Kr} deficiency contributes to the relatively depolarized resting potential of −30mV to −60mV typical of early iPSC-derived or ESC-derived cardiomyocytes. Prolonged periods of culture, augmented by signals from non-cardiomyocytes, can decrease the resting potential to about −70mV although not quite reaching the −80mV typical of adult cardiomyocytes [20, 24–27]. A consequence of the lack of a polarized resting potential is that functional Na^+ channel density is relatively low compared to more mature cells, consequently, Na^+ channel function has been inconsistent among iPSC-cardiomyocyte preparations and accounts for the slow velocities of action potential depolarization (about 2–100 V/s compared to about 300 V/s for adult ventricular cardiomyocytes [20, 24, 27].

iPSC-derived cardiomyocytes also have important differences in Ca^{2+} handling relative to adult cardiomyocytes. iPSC-cardiomyocytes have a largely undeveloped transverse tubule (T-tubule) network. T-tubules are invaginations of the sarcolemma that that organize in a periodic pattern transversely to the major axis and align with Z-lines. In adult cardiomyocytes, T-tubule caveolae align with the sarcoplasmic reticulum (SR) [28]. Action potentials trigger influx of Ca^{2+} across the sarcolemma via voltage-gated L-type Ca^{2+} channels located at the T-tubular network in close proximity to the SR. Following the action potential depolarization of the cellular membrane, the influx of extracellular Ca^{2+} triggers the rapid release of Ca^{2+} from the SR through Ryanodine receptors (RyR) in a mechanism termed calcium-induced calcium release (CICR) to rapidly coordinate the action potential with contraction. The relative contribution of the extracellular and SR Ca^{2+} pools, however, to intracellular Ca^{2+} depends on the degree of cardiomyocyte maturity, as reviewed [22, 23]. CICR dominates in mature cells that have a functional caveolae/T-tubule network, whereas influx from the extracellular pool, which slowly enters the cytoplasm, predominates in immature cardomyocytes. The slow Ca^{2+} response to electrical stimulation accounts for the negative force-frequency relationship in ESC-derived cardiomyocytes when paced, whereas adult CMs show a positive force-frequency relationship [29, 30].

Importantly, in healthy adult cardiomyocytes, the ability of adrenergic signaling to regulate Ca^{2+} handling and Ca^{2+} triggered contraction is tightly localized by the T-tubule network. Comparmentalization localizes adrenergic control of Ca^{2+} entry, Ca^{2+} release from the sarcoplasmic reticulum and its reuptake by the sarcolemma localized ATPase Ca^{2+} pump SERCA2 (ATP2A2), as well as phosphorylation of cardiac Troponin-T and phospholamban. This process is mediated by structural restriction of β2 adrenergic receptors (β2-ARs) to caveolae/T tubules [31] and by localized activity of cAMP-hydrolyzing phosphodiesterases (PDEs) [32]. Unlike healthy adult cardiomyocytes, immature iPSC-cardiomyocytes especially when cultured on unpatterned substrata (e.g. cell culture plastic) exhibit dysregulated catecholamine-dependent phosphorylation of cardiac Troponin-I and phospholamban and regulation of CAMKII [33]. Interestingly, the adrenergic regulation of the SR/Ca^{2+} handling machinery of iPSC-cardiomyocytes is somewhat reminiscent of failing cardiomyocytes. Failing adult myocytes lose T-tubule structure [34] and undergo a

switch from the normally restricted function of the β2 AR to a dysregulated β2-AR and upregulated expression of β1-ARs [35, 36], which are less sensitive to catecholamine-induced downregulation and internalization than β2-ARs [37, 38].

Little is known about the signals, either extracellular or intracellular, that direct physiological maturation of immature pluripotent stem cell derived cardiomyocytes [23]. One factor known to play a role is thyroid hormone (T3). T3 levels increase during the last trimester of human gestation and upregulates various genes encoding proteins involved in contractile and SR function, including SERCA2a and phospholamban, cardiac potassium channels, the Na^+/K^+ ATPase and NCX, as well as β-adrenergic receptors, guanine-nucleotide regulatory proteins, and adenylyl cyclases. Importantly, T3 also regulates myosin heavy chain genes at least in mice where it is responsible for the developmental shift from predominantly Myh7 in fetal to Myh6 in adult mice [39]. T3 is also reported to enhance metrics of murine ESC-cardiomyocyte maturation [40].

Interestingly, cardiac expressed microRNA miR-1 induces a phenotype trending towards electrophysiological and mechanical maturation when overexpressed in differentiated yet immature cardiomyocytes [41]. The effects include a more rapid action potential and a more hyperpolarized membrane potential. miR-1 overexpression also upregulated Kir2.1, Kv1.4, HERG and dihydropyridine receptors (VGCC; voltage-gated calcium channels) while downregulating HCN4. miR-1 overexpression also increased proteins involved in CICR and was accompanied by an increased amplitude and upstroke velocity of the Ca^{2+} transient.

Recent attempts to induce maturation by culturing iPSC-cardiomyocytes on 2-dimensional (2D) micropatterned surfaces have shown promising effects on mechanical and electrophysiological maturation and pharmacological responsiveness [42]. For instance, cardiomyocytes on 2D micropatterned arrays conform to the shape of the patterned extracelllar matrix protein (e.g. fibronectin) [43] or nanopatterned grooved surfaces [44, 45]. In addition, two recent studies [33, 46] showed that 7:1 rectangular shape might be optimal for force generation and T-tubule structure and localized adrenergic signaling. Such surfaces might represent the nearest term improvements in current culture substrata for high throughput screening since they should be adaptable to standard 96 and 384-well format, although commercial solutions do not yet exist. As a further advance, combining more elastic substrata with micropatterned and matrix protein-functionalized surfaces should enhance morphological, physiological and mechanical properties of iPSC-cardiomyocytes, including organization of the sarcomeres themselves, sarcoplasmic reticulum and T-tubule network, increased number and localization of mitochondria, resulting in enhanced force generation and a mature adrenergic responsiveness (Figure 1) [33, 46].

3D engineered heart tissues (EHTs) offer an additional level of sophistication, reviewed in [47, 48]. iPSC-cardiomyocytes are influenced by the shape such that cell alignment and degree of mechanical and morphological maturation can be controlled by molds used to cast 3D EHTs. In addition to shape, parameters evaluated in 3D EHTs include matrix material, electrical pacing, cyclical mechanical stretching, and presence of non-cardiomyoyctes, such that matrices made with collagen or fibrin and introduction of fibroblasts yields EHTs in which iPSC-cardiomyocytes achieve an impressive degree of sarcomeric, sarcoplasmic

reticulum/T-tubule and mitochondrial ultrastructural organization. Exciting advances will include creating complex, perfused 3D tissues to enhance fidelity of intercellular interactions and force generation, perhaps through innovative casting of tissues with channels that can be vascularized [49–51]. In an interesting application, monoaxial EHTs have been shown to reproduce re-entry arrhythmia [48]. In this case, normal rhythmic contraction and propagation of Ca^{2+} waves were restored by electrical shocking, stimulating restoration of sinus rhythm by resynchronization therapy.

In summary, iPSC-cardiomyocytes hold immense promise for disease modeling, even if the degree of functional maturation remains a challenge. Micropatterned surfaces seems to offer the nearest term advancement in improving iPSC-cardiomyocyte maturation, and systems with physiologically appropriate substrate elasticity advance the fidelity of iPSC-cardiomyocytes, and 3D EHTs are already showing promise.

Physiological readout modalities

Optical recording modalities have gained popularity in recent years for moderate to high throughput applications, such as library screening, to overcome the limitations of direct electrophysiological recording of cardiomyocyte transmembrane voltage and current transients. Optical recording can be done using either a kinetic plate reader (e.g. Molecular Devices FLIPR or Hamatsu FDSS7000) or a high content (imaging) platform (e.g. Vala IC200) instrumentation (Table 2). Moderate to high throughput optical modalities have been developed for four parameters of cardiomycoyte physiology: dynamic measurements of the intracellular Ca^{2+} concentration, real-time recordings of the transmembrane voltage changes, as well as cardiomyocyte sarcolemmal membrane motion (summarized in Table 2) as well as force generation (albeit with lower throughput) by traction on substrata or displacement of posts (see below). Here we will focus on the use of optical voltage and Ca^{2+} probes, multi-electrode array and impedance-measuring instruments, followed by optical measurements of motion and force suited to high throughput applications.

Fluorescent and luminescent Ca^{2+} indicators are widely used for screening in drug discovery. Since intracellular Ca^{2+} concentration changes from hundreds of nanomolar to millimolar concentrations, real-time monitoring represents a convenient and reliable way to assess cardiomyocyte activity. Fluorescent Ca^{2+} readouts are often used as a surrogate marker for a cellular events not directly involving intracellular Ca^{2+} changes [52–54]. A wide selection of commercially available organic fluorescent Ca^{2+} indicators with excellent dynamic range of a fluorescent signal (up to 30× fold relative change in fluorescence, $\Delta F/F$) and chemistries enable the probes to be readily loaded into cells, making Ca^{2+}-sensitive fluorophores a drug discovery workhorse [55–57].

Small molecule voltage sensor probes (VSPs) are lipophilic fluorescent molecules that bind to the cell membrane and alter their emission properties in response changes in a transmembrane voltage potential as the membrane depolarizes. Aminonaphthylethenylpyridinium (ANEP) dyes, such as di-4-ANEPPS, di-8-ANEPPS, as a class were first described by Loew and colleagues. [58] and recent versions have very fast response times (ns) but relatively low change in fluorescence (1–10% $\Delta F/F$ per 100mV). The

structure of these probes causes the chromophores to orient perpendicularly to the aqueous interface of the plasma membrane, where the change in transmembrane potential with depolarization is thought to shift the electron density along the probes' axis and cause a spectral shift in its fluorescent emission [59]. This electrochromic effect is very fast and sensitive. Consequently, electrochromic probes have enjoyed widespread use to measure action potentials in the context of the whole heart, in cell culture and also in combination with Ca^{2+}measurements [60]. A different mechanism is used by fluorescence resonance energy transfer (FRET) VSPs, which consist of a mobile lipophilic anion acceptor in the membrane interior and a donor located on the extracellular surface of the plasma membrane. The FRET signal induced in response to depolarization can be 33–75% per 100mV with substantially slower time constants [61].

A conceptually different small molecule voltage probe is VF2.4Cl developed by Miller et al., [62] and sold commercially as FluoVolt. VF2.4Cl is a fairly fast (sub-millisecond) small molecule voltage probe that has a large dynamic range (ΔF/F in excess of 25% per 100 mV) that overcomes the dynamic range limitations of the electrochromic dyes. The chromophore of this "molecular wire" probe is localized on the membrane surface but is quenched by electron transfer at polarized (cardiomyocyte resting) potentials, and depolarization disrupts electron transfer through the "molecular wire" causing dequenching of the chromophore. We have used Vala Sciences Kinetic Imaging Cytometer HCS platform to optically acquire voltage data from iPSC-cardiomyocytes loaded with VF2.4Cl. Camera acquisition speeds can be up to 100 frames per second using the entire detection chip, and up to 1500 frames per second with partial chip use. Given the storage and computational load at higher frame rates, the rate is adjusted to match the speed to the physiological parameter being measured [63]. Individual peak data are acquired on a cell-by-cell basis or can be acquired as a whole well ensemble average. Loess regression can be used to fit action potential peaks to individual peak data. Various metrics are calculated (action potential duration at 50 and 90% peak height, peak and decay times, V_{max} values, and the decay constant Tau).

An alternative to small molecule voltage probes is a fluorescent protein that can be engineered to respond to changes in transmembrane potential. Since such protein probes are genetically encoded, they can be stably expressed in cells overcoming limitations of dye loading and loss inherent with small molecule probes. Siegel and Isacoff [64] fused GFP to the Shaker voltage-sensitive K^+ channel to construct an early generation probe that was shown to be effective for measuring transmembrane voltage in single cells. Since then, a promising approach has been to fuse the voltage sensing phosphatase of *Ciona intestinalis* to variants of fluorescent proteins. A clear advantage of protein VSPs is that they can be used in vivo, as exemplified recently in a transgenic mouse engineered to express a *Ciona intestinalis* phosphatase-based FRET VSP selectively in cardiac myocytes [65]. Optical cardiograms were recorded ex vivo, as well as in vivo using minimally invasively fiber optics at physiological heart rates (10 Hz) and under pacing-induced arrhythmia. A promising non-FRET VSP based on the *Ciona intestinalis* phosphate is ArcLight, which confers voltage sensitivity on a pH responsive variant of eGFP known as super-ecliptic pHluorin that has a large response amplitude (−30% ΔF/F per 100mV) [66]. ArcLight has been expressed either stably or by transient lentiviral transduction into iPSC-cardiomyocytes and shown to accurately reflect the action potential prolonging effects of benchmark

compounds including dofetilide (blocks I_{Kr}), E-4031 (blocks I_{Kr}), Chromanol 293B (blocks I_{Ks}) and ATX-II (opens I_{NaL}) opening the door to rapid phenotyping of disease model iPSC-cardiomyocytes and facilitating drug screening [67, 68]. Although the fluorescence intensity of ArcLight in iPSC-cardiomyocytes correlates well with patch clamp recordings for measuring action potential duration [68], the probes have a relatively slow response time that probably preclude measuring rates during the rapid depolarization (phase 0) of the action potential, and whether the expression of the fluorescent proteins will adversely affect cardiomyocyte physiology remains an open question. Nonetheless, genetically encoded voltage probes will likely be a powerful tool for screening applications, especially since more recent variations of the approach improve the response speed, for instance by using a circularly permuted GFP [69], or by mutating the voltage-sensing phosphatase protein [70].

An important alternative to optical recording are Multi-Electrode Array (MEA) devices, which use electrodes embedded in the cell culture dish to stimulate and measure extracellular field potential waveforms induced by relatively large numbers of cardiomyocytes. These devices can record for prolonged periods of time, without inflicting mechanical damage to the cell culture. Different from patch clamp or optical methods above, the MEA electrical recording is a waveform that correlates with the cardiac action potential duration and the QT interval of *in vitro* and *in vivo* ECG and is composed of an initial rapid spike corresponding to Na^+ influx and depolarization, a slow wave/plateau phase corresponding to Ca^{2+} influx, followed by a repolarizing wave that corresponds to K^+ efflux and repolarization [71, 72]. Prolonged recording and the existence of multiwell platforms make the technology ideal for studying both the acute activity and long-term effects of ion channel modulators on electrical activity [73, 74].

A commercially available platform (iCELLigence, ACEA Biosciences) uses impedance analysis for moderate throughput measurement of cardiomyocyte contractility in physiological conditions. Cell displacement during cardiomyocytes contraction is measured as variations in impedance that directly correlates with beating frequency. As an example, impedance measurements of contractility can reveal responses to growth factors or other molecules that signal through mechanisms other than ion channels [75, 76]. Furthermore, impedance quantification of cell adhesion and spreading also contributes to an assessment of overall cell toxicity [77–80]. The recently released Cardio ECR platform (ACEA Biosciences) combines MEA and contractility recording for a simultaneous comprehensive evaluation of the excitation-contraction coupling paradigm [81].

Quantifying Contractility

Until recently, there has been a lack of methods for high-throughput assessment of cardiomyocyte contractility, due to the difficulty of quantifying cellular contractile forces and fractional shortening in a platform that recapitulates the *in vivo* myocardial microenvironment. The additional challenges associated with fabricating the plates and automating the analysis processes, and scaling them to high throughput platforms, have further complicated the development of high-throughput contractility assays.

Muscular thin film (MTF) assays [82–84] have emerged as one of the pioneering assays to quantify cardiomyocyte contractility. In these assays, a layer of cells is cultured on a polydimethylsiloxane (PDMS) elastomer thin film. Prior to measuring contractility, one edge of the PDMS film is let stand free so that systolic shortening of cardiomyocytes causes bending of the MTF. The overall contractile force developed by the beating cells is calculated by measuring the MTF radius of curvature. This platform offers versatility to control cellular organization by micropatterning cardiomyocytes on the PDMS. It also provides control over microenvironment properties such as stiffness and geometry (planar vs. curved). However, the platform offers little information about the spatial distribution of mechanical stresses within the cell layer. Finally, the manufacturing of MTFs is relatively complicated and currently costly, which could be a limiting factor in a high-throughput context.

Some of these limitations are addressed by Dynamic Monolayer Force Microscopy (DMFM, [85], which was developed to measure the spatiotemporal distribution of the cumulative mechanical stresses created by beating cardiomyocyte layers. In DMFM, cells are plated on an elastic polyacrylamide (PA) hydrogel seeded with fluorescent microspheres. When the cardiomyocytes beat, their contraction and relaxation lead to cyclic deformations of the substratum that can be determined during several cycles by tracking the displacements of the microspheres [86]. The traction stresses exerted by the cells on the substratum can be recovered from the measured deformation using traction force microscopy [87, 88]. Then, the intracellular stress distribution is calculated by solving the equations of mechanical equilibrium for a thin elastic plate subject to the reaction forces created by PA gel on cells, which are opposite to the measured traction stresses [89, 90]. DMFM provides high-resolution spatial information and is grounded on fundamental equations of continuum mechanics. Thus, it provides contraction metrics with a clear biomechanical significance (e.g axial stress, shear stresses, stresses anisotropy, etc.). However, it relies on several assumptions that need further validation, such as that the cell layer has uniform thickness and Young’s modulus. Because DMFM employs flexible PA gels, this technique offers control over cell organization and substratum stiffness via the same methods used for single cells [46]. Nevertheless, the challenges of fabricating multi-well arrays of microsphere-doped PA gels could limit the throughput of this technique.

Recent efforts have been directed towards improving processing speed and automation by directly measuring cell motion in bright field video sequences of beating cells. In contrast to MTF or DMFM assays, these methods provide surrogate metrics of contractile cell shortening instead of quantifying contractile forces. One option to achieve this goal is to determine cell deformations by optical flow analysis of microscopy bright field image sequences of beating cells [91, 92]. The resulting data are further analyzed by principal component analysis [11] or by semi-automated identification of beating centers [12] in order to derive metrics of contractile cell shortening. A simpler, more computationally efficient approach consists of determining the loss of correlation coefficient between different images along the time sequence as a metric of the overall amount of cell motion [93]. This family of methods offers relatively high throughput at the expense of diminished ability to interpret the biomechanical significance of the derived contraction metrics.

Next-generation contractility assays should integrate the high-throughput potential of direct cell motion measurements with continuum mechanics to provide contractile metrics with clear physiological meaning. With this idea in mind, we are developing protocols to measure contractility from deformation vector maps in cells that are labeled with fluorophore-conjugated wheat germ agglutinin (WGA) (Figure 2 and our unpublished results). The WGA fluorescent pattern consists of fine speckles giving a chicken-wire appearance. When the cardiomyocytes beat, their contraction and relaxation lead to cyclic motions of the speckles that can be determined using image particle image velocimetry (PIV, [94]). PIV provides similar results when compared to optical flow [14] but PIV algorithms are significantly faster, offering great potential for boosting processing speed in a high-throughput screening context. Using the cell deformation vector maps obtained from PIV, we apply Gauss' divergence theorem to automatically quantify cell contractility at low computational cost as the relative change in area of the beating cells. This novel metric can be shown to be proportional to the intracellular axial stress obtained from DMFM.

Genetic disease models

An increasing number of genetic heart diseases have been modeled through the production of patient iPSC-cardiomyocytes. To date, the culture systems used to model disease have consisted of nearly pure iPSC-cardiomyocyte cultures, and therefore have been amenable to disease in which the mutation affects cardiomyocyte function cell-autonomously, as opposed to an indirect effect of a primary dysfunction in another cell type.

Not surprisingly, arrhythmia disorders were among first to be modeled, most without a structural defect, including Long QT syndromes LQT1 (KCNQ1), 2 (KCNH2), 3 (SCN5A), and 8 (CACNA1c); and Catecholaminergic polymorphic ventricular tachycardia, CPVT (RyR or Casq2) [95]. There has been a successful modeling of arrhythmogenic right ventricular cardiomyopathy (ARVD/C, involving desmosomal protein plakoglobin), which has an associated structural defect [96, 97]. Genetic cardiovascular disease modeling using iPSC-cardiomyocytes has been reviewed recently [98–100]. Examples include familial myopathies that affect a range of sarcomere proteins and phospholamban and recapitulate Ca^{2+} transient, contractility and cell size (HCM) defects, as well as LEOPARD syndrome (PTPN11) that recapitulate cell size defects.

Modeling metabolic disease

Metabolic effects on heart function are an important area for disease modeling given that metabolic dysfunction is a large and increasing global health and economic problem. Metabolic syndrome, obesity, and type 2 diabetes are multifactorial risk factors for heart disease that make it immensely challenging to tease apart interacting gene effects in humans or animal models [101–104]. On the one hand, cardiometabolic diseases due to monogenic enzyme deficiencies have well-established clinical outcomes and cell automous pathologies that are amenable to iPSC modeling. However, they also include complex polygenic diseases such as the cardiometabolic syndrome for which culture systems consisting of single or few cell types cannot recapitulate the range of pathologies. The challenges of modeling cardiometaboic diseases has been reviewed recently [105].

Lipotoxicity is one form of cardiomyopathy amenable to iPSC cardiomyocyte modeling. For example, neutral lipid storage disease (NLSD) is a rare disorder characterized by excessive accumulation of neutral lipids in a variety of cell types in the body, including cardiomyocytes [106]. One form of NLSD with myopathy (NLSD-M) is caused by a deficiency in the patatin-like phospholipase domain-containing protein 2 (*PNPLA2)* gene encoding adipose triglyceride lipase (ATGL). ATGL hydrolyzes triacylglycerol (TAG) into diacylglycerol and free fatty acids, and patients with the deficiency accumulate lipids in both myocardium and coronary arteries. The cardiomyopathy of NLSD-M is well-suited for iPSC cardiomyocyte disease modeling given its cell-autonomously acting genetic defect and its consistent phenotype of increased lipid accumulation in cardiomyocytes. Normal patient iPSC-cardiomyocytes cultured with linoleic acid/oleic acid/bovine serum albumin (L-O-BSA) complex accumulate adiposomes (neutral lipid droplets) readily visible and quantifiable by nile red staining (Figure 3). To model the deficiency, knock down of PNPLA2 by siRNA transfection caused an increase in adiposome formation, as quantified by high content microscopy. Adiposome formation was further increased by culture under hypoxia, which decreases metabolism of intracellular fat stores. Assays using this simple assay will enable high throughput evaluation of susceptibility loci by loss (e.g. siRNA knockdown) and gain (e.g. ORF expression) of function screens.

Modeling alternans and pro-arrhythmic risk

In addition to genetic disease, dysregulation of physiology is also apparent and can be evaluated in response to reference compounds. Modeling cellular bases for prolongation of the QT interval, which on the electrocardiogram (ECG) is a non-invasive marker of increased risk of sudden cardiac death (SCD) and fatal arrhythmia from drug side effects [107]. The cellular manifestation is a prolongation of the action potential duration (APD) and after depolarizations. Pro-arrhythmia risk has been a major reason for failure of drugs during development in particular the risk of drug-induced long QT and fatal polymorphic ventricular tachycardia “torsades de pointes” (TdP) [108]. Notable examples include the 1992 US FDA request for a black box warning for terfenadine, a non-sedating antihistamine for the treatment of allergic rhinitis. Ultimately, the FDA requested withdrawal from the market in 1997. Other notable instances include the serotonin agonist, cisapride, which was marketed by Janssen-Ortho and caused 125 deaths before its use ceased, propoxyphene, an opioid pain reliever marketed by Xanodyne Pharmaceuticals, and Sibutramine, a weight loss drug from Abbott Laboratories. In addition to the injury to the patients, withdrawals are extremely damaging to the companies involved given that the cost to develop a new drugs could be $2 billion [109, 110].

Arrhythmic risk is associated with binding to and inhibition of the hERG K^+ channel, encoded by *KCNH2*, and inhibition of the delayed rectifier current I_{Kr} since the outward flow of K^+ is largely responsible for the kinetics of phase 4 repolarization of the action potential. Following the documented hERG block and arrythmogenicity of drugs such as terfenadine, testing for hERG inhibition is embodied in regulatory guidelines for drug development [111]. Although hERG testing has prevented drugs at risk for TdP from entering the market, hERG binding *per se* is not entirely predictive of arrhythmia or QT prolongation, since modulation of other ion channels (e.g. blocking inward flow of Ca^{2+})

can mitigate the effects of blocking the outward flow of K^+ [112, 113]. For instance, whereas I_{Kr} blockers such as sotalol and dofetilide cause lethal arrhythmia, other I_{Kr} blockers such as verapamil elicit a far lower incidence of TdP, probably because of simultaneous blockade of L-type Ca^{2+} channels and the inward flux of Ca^{2+} [114, 115]. Similarly, ranolazine, also an I_{Kr} blocker, does not prolong the QT interval, most likely reflecting its block of I_{NaL} [116]. Thus, multiple mechanisms maintain normal repolarization, leading to the concept of "repolarization reserve" [117] that can be reduced to a threshold for QT prolongation by combined effects of drugs and other stressors, such as slow heart rates or hypokalemia.

Confounding things further, substantial differences in drug responsiveness between species can limit the effectiveness of predicting clinical outcome from animal toxicity testing [118, 119]. Nonethless, for cardiac safety and pro-arrhythmia risk assessment, animal testing, especially using sophisticated models such as animals with chronic AV block to reduce repolarization reserve [120], is considered predictive and remains the standard pre-clinical model [121]. These models are expensive and complicated to implement, however, at early stages of the development pipeline. Therefore, iPSC-cardiomyocytes are of considerable interest in modeling drug-induced arrhythmia since they represent a facile model of the integrated response to multiple cardiac ion channels and currents in a human cell context. Furthermore, patient-specific cells would open the door to investigate individual patient susceptibility to drug-induced arrhythmia.

There have been a number of reports using a variety of readout modalities (see below) to measure pro-arrhythmia risk using iPSC-cardiomyocytes. Patch-clamp and membrane potential analysis are considered the gold standard for the analysis of proarrhythmia risk as part of cardiotoxicity assessment given the conceptual association between action potential duration, after-depolarizations and QT prolongation. Ca^{2+} transient kinetics integrate the effects of multiple channels and, in addition to voltage, have been used to create pro-arrhythmia risk indices, for instance see [122] A physiological rationale for using Ca^{2+} transient kinetic analysis is that cyclic beat-to-beat variations in contraction amplitude (mechanical alternans), action potential duration (APD or electrical alternans), and cytosolic Ca^{2+} transient (Ca^{2+} transient alternans) amplitude at constant stimulation frequency are the cellular manifestation of cardiac alternans [123]. At the ECG level, cardiac T-wave alternans is the cyclical beat-to-beat fluctuation in the shape and amplitude of the ST segment or the T wave [124]. T-wave alternans has proven to be predictive risk for cardiovascular mortality, including sudden cardiac death [125]. The relationship between pacing-induced action potential duration and Ca^{2+} transient alternans was studied recently in single rabbit atrial and ventricular myocytes using combined intracellular Ca^{2+} concentration $[Ca^{2+}]i$ and electrophysiological measurements [126]. This study found that $[Ca^{2+}]i$ alternans correlated in time and magnitude with action potential alternans. Moreover, eliminating intracellular Ca^{2+} release abolished action potential alternans, but alternation of the voltage command did not affect Ca^{2+} alternans. These data suggest that a primary disturbance in Ca^{2+} handling might give rise to cellular manifestations of alternans.

Modeling cardiotoxicity

As for arrhythmic risk, cardiotoxic and myopathic effects of drugs can in theory be modeled using iPSC-cardiomyocytes. The potential exists to correlate drug dosing and plasma concentrations with cardiotoxic and myopathic risk. Recent studies suggest that iPSC-cardiomyocytes can reveal cardiotoxicities manifesting as alterations in cardiomyocyte viability, contractility, intracellular signaling and gene expression [127, 128]. As above, however, there is great need for validation, especially considering that many anti-cancer drugs elicit their cardiac effects by affecting mitochondrial function [129, 130] and that iPSC-cardiomyocytes are metabolically immature [131]. Furthermore, it will be important to evaluate the influence that patient-to-patient variation has on drug effects, as well as differences in production and culture protocols on anti-cancer drug effects is largely unexplored.

Progress towards adopting iPSC-cardiomyocytes for cardiac safety assessment

The current safety testing paradigm is based on the idea that drug-induced hERG channel blockade *in vitro* is predictive of clinical QT interval prolongation and the lethal TdP ventricular tachycardia [111]. Consequently, the now common hERG testing embodied in governmental guidelines has largely prevented new drugs with unanticipated potential for torsade from entering the market. On the other hand, reliance on hERG testing might have halted development of potentially useful therapeutics. In 2013, the US Food and Drug Administration convened a consortium of academics, governmental regulators and industry practitioners that concluded that there is a significant need for more predictive pro-arrhythmia risk tests to replace the current practices, and suggested a new paradigm for testing that integrates non-clinical in vitro and in silico approaches [111]. The new paradigm, termed Comprehensive In Vitro Proarrhythmia Assay (CiPA), is intended to revise tests for hERG blockade and possibly replace thorough QT (TQT) studies to more accurately predict arrhythmogenic compounds and diminish detection of false positives.

Despite their obvious advantages, it seems too soon to tell when (or if) iPSC-cardiomyocytes will play an important role in arrhythmogenic risk assessment. Given their relative physiological immaturity and the multiple protocols for producing and culturing iPSC-cardiomyocytes, as well as readout modalities, there is a great need to validate their use through testing of panels of compounds with safe and pro-arrhythmic profiles. Such a panel of drugs has recently been released as part of the CiPA initiative. Testing a range of cells and culture conditions is underway in independent laboratories. With respect to the iPSC-cardiomyocytes themselves, their reported differences (as discussed above) in electrophysiological phenotypes might be related to differences in iPSC generation, protocols for cardiomyocyte preparation, a natural heterogeneity in the cardiomyocyte types (e.g. ventricular, atrial, nodal in the cultures), and degree of maturation, necessitating substantial effort to standardize experimental conditions.

Patient background is an important concern as well, both for defining a normal individual, as well as for the possibility of incorporating iPSC-cardiomyocytes from patients harboring

genetic mutations or polymorphisms that increase susceptibility to drug-induced arrhythmia. It will be necessary to resolve the challenges laid out above before panels of at-risk patient iPSC-cardiomyocytes might yield assays with predictive power exceeding that of clinical testing and amenable for early stage drug development [132].

A wish list to improve disease modeling using iPSC-cardiomyocytes

The following is a short list of advances that we feel would increase the utility of iPSC-cardiomyocytes for elucidating disease mechanisms and use in drug discovery:

- Improving maturity. Culture methods to improve the electrophysiological, mechanical and metabolic maturity of iPSC-cardiomyocytes is likely to top the list of desired advances. Maturity affects predictiveness and is related to all of the issues below. Research is needed into paracrine signaling, possible influence of non-cardiomyocytes and extracellular matrix, substrate stiffness and metabolism.
- Improving directed differentiation. Depending on the differentiation protocol and even the iPSC line, there is significant variability in the proportion of different types of cardiomyocytes, including variation in the representation of ventricular-like, atrial-like, pacemaker-like. Consequently, most of the model systems are not homogenous. This problem, like the cell maturity issue (above), compromise the fidelity of iPSC-cardiomyocytes as models of the human condition. Although to a degree this might be alleviated by sorting, it is in our view preferable to define signals, informed by embryology, that direct differentiation of distinct cardiomyocyte subtypes.
- Cell systems/substrates reveal physiological regulation and perturbation of contraction and relaxation. Substrata with tissue-appropriate stiffness and analysis methods leading to traction force measurements in high throughput might be useful to reveal the effects of new generation of drugs that target the sarcomere [133]. Towards this end, Mathur et al. [134] have created a 3D microfluidics chamber with cardiomyocytes cultured on micropatterned surfaces to induce anisotropy and alignment.
- EHTs that mimic multicellular basis for arrhythmia and more faithfully recapitulate alterations in contraction and relaxation kinetics in disease and in response to drugs.

We expect the above advances to be achievable in the near-term. Among longer term advances that would increase utility would be 3D EHTs that incorporate microvascular system to perfuse the muscle allowing the development of thicker and more realistically patterned tissues to recapitulate aspects of the ventricular wall [50, 51]. Such advances might be useful to model challenging problems, such as failure of the right ventricle that that can occur in congenital hypoplastic left heart following corrective surgery [135, 136].

In summary, in iPSC-cardiomyocyte biology coupled to high throughput instrumentation and physiological probes have the potential to re-introduce the human context into the earliest stages of cardiac drug discovery. Furthermore, phenotypic, disease-specific assays

screened against focused libraries allow the entire proteome to be interrogated to discover candidate therapeutic targets representing a powerful paradigm shift in drug discovery.

Acknowledgments

We wish to acknowledge grant support from the NIH (1R01HL128072 and 5R01 HL113601 to MM, and 1R01 GM084227 to JCdA), the California Institute for Regenerative Medicine (CIRM TR4-06857 and CIRM RB5-07356 to MM), the Fondation Leducq Shapeheart Transatlantic Alliance, and a National Science Foundation Chemical, Bioengineering, Environmental, and Transport Systems (CBET) grant (1055697) to JCdA.

References

1. Balinsky BI. Experiments on total extirpation of the whole endoderm in *Triton* embryos. C.r Acad Sci URSS. 1939; 23:196–198.
2. Chuang HH, Tseng MP. An experimental analysis of the determination and differentiation of the mesodermal structures of neurula in urodeles. Scientia Sinica. 1957; 6:669–708. [PubMed: 13519126]
3. Jacobson AG. Influences of ectoderm and endoderm on heart differentiation in the newt. Developmental Biology. 1960; 2:138–154. [PubMed: 14406400]
4. Jacobson AG. Heart determination in the newt. Journal of Experimental Zoology. 1961; 146:139–152. [PubMed: 14450715]
5. Nieuwkoop PD. Experimental investigations on the origin and determination of the germ cells, and on the development of the lateral plates and germ ridges in Urodeles. Archs Neerl Zool. 1947; 8:1–205.
6. Sater AK, Jacobson AG. The specification of heart mesoderm occurs during gastrulation in *Xenopus laevis*. Development. 1989; 105:821–830. [PubMed: 2598816]
7. Nascone N, Mercola M. An inductive role for the endoderm in *Xenopus* cardiogenesis. Development. 1995; 121:515–523. [PubMed: 7768189]
8. Sater AK, Jacobson AG. The role of the dorsal lip in the induction of heart mesoderm in *Xenopus laevis*. Development. 1990; 108:461–470. [PubMed: 2340810]
9. Orts-Llorca F. Influence of the endoderm on heart differentiation during the early stages of development of the chicken embryo. Wilhelm Roux Arch EntwMech Org. 1963; 154:533–551.
10. Orts-Llorca F, Gil DR. Influence of the endoderm on heart differentiation. Wilhelm Roux ARch EntwMech Org. 1965; 156:368–370.
11. Schultheiss TM, Xydas S, Lassar AB. Induction of avian cardiac myogenesis by anterior endoderm. Development. 1995; 121:4203–4214. [PubMed: 8575320]
12. Schneider VA, Mercola M. Wnt antagonism initiates cardiogenesis in Xenopus laevis. Genes Dev. 2001; 15:304–315. [PubMed: 11159911]
13. Marvin MJ, Di Rocco G, Gardiner A, Bush SM, Lassar AB. Inhibition of Wnt activity induces heart formation from posterior mesoderm. Genes Dev. 2001; 15:316–327. [PubMed: 11159912]
14. Meganathan K, Sotiriadou I, Natarajan K, Hescheler J, Sachinidis A. Signaling molecules, transcription growth factors and other regulators revealed from in-vivo and in-vitro models for the regulation of cardiac development. Int J Cardiol. 2015; 183:117–128. [PubMed: 25662074]
15. Willems E, Spiering S, Davidovics H, Lanier M, Xia Z, Dawson M, Cashman J, Mercola M. Small-molecule inhibitors of the Wnt pathway potently promote cardiomyocytes from human embryonic stem cell-derived mesoderm. Circ Res. 2011; 109:360–364. [PubMed: 21737789]
16. Kattman SJ, Witty AD, Gagliardi M, Dubois NC, Niapour M, Hotta A, Ellis J, Keller G. Stage-Specific Optimization of Activin/Nodal and BMP Signaling Promotes Cardiac Differentiation of Mouse and Human Pluripotent Stem Cell Lines. Cell Stem Cell. 2011; 8:228–240. [PubMed: 21295278]
17. Zhu WZ, Van Biber B, Laflamme MA. Methods for the derivation and use of cardiomyocytes from human pluripotent stem cells. Methods Mol Biol. 2011; 767:419–431. [PubMed: 21822893]

18. Lian X, Zhang J, Azarin SM, Zhu K, Hazeltine LB, Bao X, Hsiao C, Kamp TJ, Palecek SP. Directed cardiomyocyte differentiation from human pluripotent stem cells by modulating Wnt/beta-catenin signaling under fully defined conditions. Nat Protoc. 2013; 8:162–175. [PubMed: 23257984]
19. Burridge PW, Keller G, Gold JD, Wu JC. Production of de novo cardiomyocytes: human pluripotent stem cell differentiation and direct reprogramming. Cell Stem Cell. 2012; 10:16–28. [PubMed: 22226352]
20. Ma J, Guo L, Fiene SJ, Anson BD, Thomson JA, Kamp TJ, Kolaja KL, Swanson BJ, January CT. High purity human-induced pluripotent stem cell-derived cardiomyocytes: electrophysiological properties of action potentials and ionic currents. American journal of physiology. Heart and circulatory physiology. 2011; 301:H2006–2017. [PubMed: 21890694]
21. Hoekstra M, Mummery CL, Wilde AA, Bezzina CR, Verkerk AO. Induced pluripotent stem cell derived cardiomyocytes as models for cardiac arrhythmias. Front Physiol. 2012; 3:346. [PubMed: 23015789]
22. Knollmann BC. Induced pluripotent stem cell-derived cardiomyocytes: boutique science or valuable arrhythmia model? Circ Res. 2013; 112:969–976. discussion 976. [PubMed: 23569106]
23. Keung W, Boheler KR, Li RA. Developmental cues for the maturation of metabolic, electrophysiological and calcium handling properties of human pluripotent stem cell-derived cardiomyocytes. Stem Cell Res Ther. 2014; 5:17. [PubMed: 24467782]
24. Kim C, Majdi M, Xia P, Wei KA, Talantova M, Spiering S, Nelson B, Mercola M, Chen HS. Non-cardiomyocytes influence the electrophysiological maturation of human embryonic stem cell-derived cardiomyocytes during differentiation. Stem Cells Dev. 2010; 19:783–795. [PubMed: 20001453]
25. Pekkanen-Mattila M, Ojala M, Kerkela E, Rajala K, Skottman H, Aalto-Setala K. The effect of human and mouse fibroblast feeder cells on cardiac differentiation of human pluripotent stem cells. Stem Cells Int. 2012; 2012:875059. [PubMed: 22315618]
26. Zhang Q, Jiang J, Han P, Yuan Q, Zhang J, Zhang X, Xu Y, Cao H, Meng Q, Chen L, Tian T, Wang X, Li P, Hescheler J, Ji G, Ma Y. Direct differentiation of atrial and ventricular myocytes from human embryonic stem cells by alternating retinoid signals. Cell Res. 2011; 21:579–587. [PubMed: 21102549]
27. Lundy SD, Zhu WZ, Regnier M, Laflamme MA. Structural and functional maturation of cardiomyocytes derived from human pluripotent stem cells. Stem Cells Dev. 2013; 22:1991–2002. [PubMed: 23461462]
28. Ibrahim M, Gorelik J, Yacoub MH, Terracciano CM. The structure and function of cardiac t-tubules in health and disease. Proc Biol Sci. 2011; 278:2714–2723. [PubMed: 21697171]
29. Dolnikov K, Shilkrut M, Zeevi-Levin N, Gerecht-Nir S, Amit M, Danon A, Itskovitz-Eldor J, Binah O. Functional properties of human embryonic stem cell-derived cardiomyocytes: intracellular Ca2+ handling and the role of sarcoplasmic reticulum in the contraction. Stem Cells. 2006; 24:236–245. [PubMed: 16322641]
30. Poon E, Kong CW, Li RA. Human pluripotent stem cell-based approaches for myocardial repair: from the electrophysiological perspective. Mol Pharm. 2011; 8:1495–1504. [PubMed: 21879736]
31. Nikolaev VO, Bunemann M, Schmitteckert E, Lohse MJ, Engelhardt S. Cyclic AMP imaging in adult cardiac myocytes reveals far-reaching beta1-adrenergic but locally confined beta2-adrenergic receptor-mediated signaling. Circ Res. 2006; 99:1084–1091. [PubMed: 17038640]
32. Perry SJ, Baillie GS, Kohout TA, McPhee I, Magiera MM, Ang KL, Miller WE, McLean AJ, Conti M, Houslay MD, Lefkowitz RJ. Targeting of cyclic AMP degradation to beta 2-adrenergic receptors by beta-arrestins. Science. 2002; 298:834–836. [PubMed: 12399592]
33. Jung G, Fajardo G, Ribeiro AJS, Kooiker KB, Coronado M, Zhao M, Hu DQ, Reddy S, Kodo K, Sriram K, Insel PA, Wu JC, Pruitt BL, Bernstein D. Time-dependent Evolution of Functional vs. Remodeling Signaling in iPSC-derived Cardiomyocytes and Induced Maturation with Biomechanical Stimulation. FASEB J. 2015 in press.
34. Lyon AR, MacLeod KT, Zhang Y, Garcia E, Kanda GK, Lab MJ, Korchev YE, Harding SE, Gorelik J. Loss of T-tubules and other changes to surface topography in ventricular myocytes from

failing human and rat heart. Proc Natl Acad Sci U S A. 2009; 106:6854–6859. [PubMed: 19342485]

35. Nikolaev VO, Moshkov A, Lyon AR, Miragoli M, Novak P, Paur H, Lohse MJ, Korchev YE, Harding SE, Gorelik J. Beta2-adrenergic receptor redistribution in heart failure changes cAMP compartmentation. Science. 2010; 327:1653–1657. [PubMed: 20185685]
36. Kaumann A, Bartel S, Molenaar P, Sanders L, Burrell K, Vetter D, Hempel P, Karczewski P, Krause EG. Activation of beta2-adrenergic receptors hastens relaxation and mediates phosphorylation of phospholamban, troponin I, and C-protein in ventricular myocardium from patients with terminal heart failure. Circulation. 1999; 99:65–72. [PubMed: 9884381]
37. Lefkowitz RJ. G protein-coupled receptors. III. New roles for receptor kinases and beta-arrestins in receptor signaling and desensitization. J Biol Chem. 1998; 273:18677–18680. [PubMed: 9668034]
38. Rapacciuolo A, Suvarna S, Barki-Harrington L, Luttrell LM, Cong M, Lefkowitz RJ, Rockman HA. Protein kinase A and G protein-coupled receptor kinase phosphorylation mediates beta-1 adrenergic receptor endocytosis through different pathways. J Biol Chem. 2003; 278:35403–35411. [PubMed: 12821660]
39. Ojamaa K, Klemperer JD, MacGilvray SS, Klein I, Samarel A. Thyroid hormone and hemodynamic regulation of beta-myosin heavy chain promoter in the heart. Endocrinology. 1996; 137:802–808. [PubMed: 8603588]
40. Lee J, Yun MJ, Nam KH, Chung WY, Soh EY, Park CS. Quality of life and effectiveness comparisons of thyroxine withdrawal, triiodothyronine withdrawal, and recombinant thyroid-stimulating hormone administration for low-dose radioiodine remnant ablation of differentiated thyroid carcinoma. Thyroid. 2010; 20:173–179. [PubMed: 20151824]
41. Fu JD, Rushing SN, Lieu DK, Chan CW, Kong CW, Geng L, Wilson KD, Chiamvimonvat N, Boheler KR, Wu JC, Keller G, Hajjar RJ, Li RA. Distinct roles of microRNA-1 and −499 in ventricular specification and functional maturation of human embryonic stem cell-derived cardiomyocytes. PLoS One. 2011; 6:e27417. [PubMed: 22110643]
42. Parker KK, Tan J, Chen CS, Tung L. Myofibrillar architecture in engineered cardiac myocytes. Circ Res. 2008; 103:340–342. [PubMed: 18635822]
43. Sun Y, Jallerat Q, Szymanski JM, Feinberg AW. Conformal nanopatterning of extracellular matrix proteins onto topographically complex surfaces. Nat Methods. 2015; 12:134–136. [PubMed: 25506720]
44. Kim J, Park J, Na K, Yang S, Baek J, Yoon E, Choi S, Lee S, Chun K, Park J, Park S. Quantitative evaluation of cardiomyocyte contractility in a 3D microenvironment. J Biomech. 2008; 41:2396–2401. [PubMed: 18644311]
45. Kim DH, Lipke EA, Kim P, Cheong R, Thompson S, Delannoy M, Suh KY, Tung L, Levchenko A. Nanoscale cues regulate the structure and function of macroscopic cardiac tissue constructs. Proc Natl Acad Sci U S A. 2010; 107:565–570. [PubMed: 20018748]
46. Ribeiro AJ, Ang YS, Fu JD, Rivas RN, Mohamed TM, Higgs GC, Srivastava D, Pruitt BL. Contractility of single cardiomyocytes differentiated from pluripotent stem cells depends on physiological shape and substrate stiffness. Proc Natl Acad Sci U S A. 2015; 112:12705–12710. [PubMed: 26417073]
47. Hirt MN, Hansen A, Eschenhagen T. Cardiac tissue engineering: state of the art. Circ Res. 2014; 114:354–367. [PubMed: 24436431]
48. Thavandiran N, Dubois N, Mikryukov A, Masse S, Beca B, Simmons CA, Deshpande VS, McGarry JP, Chen CS, Nanthakumar K, Keller GM, Radisic M, Zandstra PW. Design and formulation of functional pluripotent stem cell-derived cardiac microtissues. Proc Natl Acad Sci U S A. 2013; 110:E4698–4707. [PubMed: 24255110]
49. Miller JS, Stevens KR, Yang MT, Baker BM, Nguyen DH, Cohen DM, Toro E, Chen AA, Galie PA, Yu X, Chaturvedi R, Bhatia SN, Chen CS. Rapid casting of patterned vascular networks for perfusable engineered three-dimensional tissues. Nat Mater. 2012; 11:768–774. [PubMed: 22751181]
50. Morgan JP, Delnero PF, Zheng Y, Verbridge SS, Chen J, Craven M, Choi NW, Diaz-Santana A, Kermani P, Hempstead B, Lopez JA, Corso TN, Fischbach C, Stroock AD. Formation of microvascular networks in vitro. Nat Protoc. 2013; 8:1820–1836. [PubMed: 23989676]

51. Sekine H, Shimizu T, Sakaguchi K, Dobashi I, Wada M, Yamato M, Kobayashi E, Umezu M, Okano T. In vitro fabrication of functional three-dimensional tissues with perfusable blood vessels. Nat Commun. 2013; 4:1399. [PubMed: 23360990]
52. Wyrsch P, Blenn C, Pesch T, Beneke S, Althaus FR. Cytosolic Ca2+ shifts as early markers of cytotoxicity. Cell Commun Signal. 2013; 11:11. [PubMed: 23384168]
53. Spencer CI, Baba S, Nakamura K, Hua EA, Sears MA, Fu CC, Zhang J, Balijepalli S, Tomoda K, Hayashi Y, Lizarraga P, Wojciak J, Scheinman MM, Aalto-Setala K, Makielski JC, January CT, Healy KE, Kamp TJ, Yamanaka S, Conklin BR. Calcium transients closely reflect prolonged action potentials in iPSC models of inherited cardiac arrhythmia. Stem Cell Reports. 2014; 3:269–281. [PubMed: 25254341]
54. Grienberger C, Konnerth A. Imaging calcium in neurons. Neuron. 2012; 73:862–885. [PubMed: 22405199]
55. Sirenko O, Crittenden C, Callamaras N, Hesley J, Chen YW, Funes C, Rusyn I, Anson B, Cromwell EF. Multiparameter in vitro assessment of compound effects on cardiomyocyte physiology using iPSC cells. J Biomol Screen. 2013; 18:39–53. [PubMed: 22972846]
56. Molokanova E, Savchenko A. Bright future of optical assays for ion channel drug discovery. Drug Discov Today. 2008; 13:14–22. [PubMed: 18190859]
57. Grimm FA, Iwata Y, Sirenko O, Bittner M, Rusyn I. High-Content Assay Multiplexing for Toxicity Screening in Induced Pluripotent Stem Cell-Derived Cardiomyocytes and Hepatocytes. Assay Drug Dev Technol. 2015; 13:529–546. [PubMed: 26539751]
58. Fluhler E, Burnham VG, Loew LM. Spectra, membrane binding, and potentiometric responses of new charge shift probes. Biochemistry. 1985; 24:5749–5755. [PubMed: 4084490]
59. Loew LM. Potentiometric dyes: Imaging electrical activity of cell membranes. Pure and Applied Chemistry. 2009; 68:1405–1409.
60. Lopez-Izquierdo A, Warren M, Riedel M, Cho S, Lai S, Lux RL, Spitzer KW, Benjamin IJ, Tristani-Firouzi M, Jou CJ. A near-infrared fluorescent voltage-sensitive dye allows for moderate-throughput electrophysiological analyses of human induced pluripotent stem cell-derived cardiomyocytes. Am J Physiol Heart Circ Physiol. 2014; 307:H1370–1377. [PubMed: 25172899]
61. Bradley J, Luo R, Otis TS, DiGregorio DA. Submillisecond optical reporting of membrane potential in situ using a neuronal tracer dye. J Neurosci. 2009; 29:9197–9209. [PubMed: 19625510]
62. Miller EW, Lin JY, Frady EP, Steinbach PA, Kristan WB Jr, Tsien RY. Optically monitoring voltage in neurons by photo-induced electron transfer through molecular wires. Proc Natl Acad Sci U S A. 2012; 109:2114–2119. [PubMed: 22308458]
63. Black, HS. Modulation Theory. Van Nostrand: Place Published; 1953.
64. Siegel MS, Isacoff EY. A genetically encoded optical probe of membrane voltage. Neuron. 1997; 19:735–741. [PubMed: 9354320]
65. Chang Liao ML, de Boer TP, Mutoh H, Raad N, Richter C, Wagner E, Downie BR, Unsold B, Arooj I, Streckfuss-Bomeke K, Doker S, Luther S, Guan K, Wagner S, Lehnart SE, Maier LS, Stuhmer W, Wettwer E, van Veen T, Morlock MM, Knopfel T, Zimmermann WH. Sensing Cardiac Electrical Activity With a Cardiac Myocyte–Targeted Optogenetic Voltage Indicator. Circ Res. 2015; 117:401–412. [PubMed: 26078285]
66. Jin L, Han Z, Platisa J, Wooltorton JR, Cohen LB, Pieribone VA. Single action potentials and subthreshold electrical events imaged in neurons with a fluorescent protein voltage probe. Neuron. 2012; 75:779–785. [PubMed: 22958819]
67. Shinnawi R, Huber I, Maizels L, Shaheen N, Gepstein A, Arbel G, Tijsen AJ, Gepstein L. Monitoring Human-Induced Pluripotent Stem Cell-Derived Cardiomyocytes with Genetically Encoded Calcium and Voltage Fluorescent Reporters. Stem Cell Reports. 2015; 5:582–596. [PubMed: 26372632]
68. Leyton-Mange JS, Mills RW, Macri VS, Jang MY, Butte FN, Ellinor PT, Milan DJ. Rapid cellular phenotyping of human pluripotent stem cell-derived cardiomyocytes using a genetically encoded fluorescent voltage sensor. Stem Cell Reports. 2014; 2:163–170. [PubMed: 24527390]

69. St-Pierre F, Marshall JD, Yang Y, Gong Y, Schnitzer MJ, Lin MZ. High-fidelity optical reporting of neuronal electrical activity with an ultrafast fluorescent voltage sensor. Nat Neurosci. 2014; 17:884–889. [PubMed: 24755780]
70. Piao HH, Rajakumar D, Kang BE, Kim EH, Baker BJ. Combinatorial mutagenesis of the voltage-sensing domain enables the optical resolution of action potentials firing at 60 Hz by a genetically encoded fluorescent sensor of membrane potential. J Neurosci. 2015; 35:372–385. [PubMed: 25568129]
71. Halbach MD, Egert U, Hescheler J, Banach K. Estimation of Action Potential Changes from Field Potential Recordings in Multicellular Mouse Cardiac Myocyte Cultures. Cellular Physiology and Biochemistry. 2003; 13:271–284. [PubMed: 14586171]
72. Guo L, Qian JY, Abrams R, Tang HM, Weiser T, Sanders MJ, Kolaja KL. The Electrophysiological Effects of Cardiac Glycosides in Human iPSC-derived Cardiomyocytes and in Guinea Pig Isolated Hearts. Cellular Physiology and Biochemistry. 2011; 27:453–462. [PubMed: 21691062]
73. Harris K, Aylott M, Cui Y, Louttit JB, McMahon NC, Sridhar A. Comparison of Electrophysiological Data From Human-Induced Pluripotent Stem Cell–Derived Cardiomyocytes to Functional Preclinical Safety Assays. Toxicological Sciences. 2013; 134:412–426. [PubMed: 23690542]
74. Navarrete EG, Liang P, Lan F, Sanchez-Freire V, Simmons C, Gong T, Sharma A, Burridge PW, Patlolla B, Lee AS, Wu H, Beygui RE, Wu SM, Robbins RC, Bers DM, Wu JC. Screening Drug-Induced Arrhythmia Using Human Induced Pluripotent Stem Cell–Derived Cardiomyocytes and Low-Impedance Microelectrode Arrays. Circulation. 2013; 128:S3–S13. [PubMed: 24030418]
75. Bornholz B, Weidtkamp-Peters S, Schmitmeier S, Seidel CA, Herda LR, Felix SB, Lemoine H, Hescheler J, Nguemo F, Schafer C, Christensen MO, Mielke C, Boege F. Impact of human autoantibodies on beta1-adrenergic receptor conformation, activity, and internalization. Cardiovascular research. 2013; 97:472–480. [PubMed: 23208588]
76. Eldridge S, Guo L, Mussio J, Furniss M, Hamre J, Davis M. Examining the Protective Role of ErbB2 Modulation in Human-Induced Pluripotent Stem Cell-Derived Cardiomyocytes. Toxicological Sciences. 2014; 141:547–559. [PubMed: 25055963]
77. Abassi YA, Xi B, Li N, Ouyang W, Seiler A, Watzele M, Kettenhofen R, Bohlen H, Ehlich A, Kolossov E, Wang X, Xu X. Dynamic monitoring of beating periodicity of stem cell-derived cardiomyocytes as a predictive tool for preclinical safety assessment. British Journal of Pharmacology. 2012; 165:1424–1441. [PubMed: 21838757]
78. Xi B, Wang T, Li N, Ouyang W, Zhang W, Wu J, Xu X, Wang X, Abassi YA. Functional Cardiotoxicity Profiling and Screening Using the xCELLigence RTCA Cardio System. Journal of the Association for Laboratory Automation. 2011; 16:415–421.
79. Guo L, Abrams RMC, Babiarz JE, Cohen JD, Kameoka S, Sanders MJ, Chiao E, Kolaja KL. Estimating the Risk of Drug-Induced Proarrhythmia Using Human Induced Pluripotent Stem Cell–Derived Cardiomyocytes. Toxicological Sciences. 2011; 123:281–289. [PubMed: 21693436]
80. Scott CW, Zhang X, Abi-Gerges N, Lamore SD, Abassi YA, Peters MF. An Impedance-Based Cellular Assay Using Human iPSC-Derived Cardiomyocytes to Quantify Modulators of Cardiac Contractility. Toxicological Sciences. 2014; 142:331–338. [PubMed: 25237062]
81. Guo L, Eldridge S, Furniss M, Mussio J, Davis M. Use of Human Induced Pluripotent Stem Cell-Derived Cardiomyocytes (hiPSC-CMs) to Monitor Compound Effects on Cardiac Myocyte Signaling Pathways. Current protocols in chemical biology. 2015; 7:141–185. [PubMed: 26331525]
82. Feinberg AW, Feigel A, Shevkoplyas SS, Sheehy S, Whitesides GM, Parker KK. Muscular thin films for building actuators and powering devices. Science. 2007; 317:1366–1370. [PubMed: 17823347]
83. Grosberg A, Nesmith AP, Goss JA, Brigham MD, McCain ML, Parker KK. Muscle on a chip: in vitro contractility assays for smooth and striated muscle. J Pharmacol Toxicol Methods. 2012; 65:126–135. [PubMed: 22521339]
84. Sheehy SP, Pasqualini F, Grosberg A, Park SJ, Aratyn-Schaus Y, Parker KK. Quality metrics for stem cell-derived cardiac myocytes. Stem Cell Reports. 2014; 2:282–294. [PubMed: 24672752]

85. Banerjee I, Carrion K, Serrano R, Dyo J, Sasik R, Lund S, Willems E, Aceves S, Meili R, Mercola M, Chen J, Zambon A, Hardiman G, Doherty TA, Lange S, del Alamo JC, Nigam V. Cyclic stretch of embryonic cardiomyocytes increases proliferation, growth, and expression while repressing Tgf-beta signaling. J Mol Cell Cardiol. 2015; 79:133–144. [PubMed: 25446186]

86. Jacot JG, McCulloch AD, Omens JH. Substrate stiffness affects the functional maturation of neonatal rat ventricular myocytes. Biophysical Journal. 2008 in revision.

87. del Alamo JC, Meili R, Alvarez-Gonzalez B, Alonso-Latorre B, Bastounis E, Firtel R, Lasheras JC. Three-dimensional quantification of cellular traction forces and mechanosensing of thin substrata by fourier traction force microscopy. PLoS One. 2013; 8:e69850. [PubMed: 24023712]

88. Del Alamo JC, Meili R, Alonso-Latorre B, Rodriguez-Rodriguez J, Aliseda A, Firtel RA, Lasheras JC. Spatio-temporal analysis of eukaryotic cell motility by improved force cytometry. Proc Natl Acad Sci U S A. 2007; 104:13343–13348. [PubMed: 17684097]

89. Hur SS, del Alamo JC, Park JS, Li YS, Nguyen HA, Teng D, Wang KC, Flores L, Alonso-Latorre B, Lasheras JC, Chien S. Roles of cell confluency and fluid shear in 3-dimensional intracellular forces in endothelial cells. Proc Natl Acad Sci U S A. 2012; 109:11110–11115. [PubMed: 22665785]

90. Tambe DT, Croutelle U, Trepat X, Park CY, Kim JH, Millet E, Butler JP, Fredberg JJ. Monolayer stress microscopy: limitations, artifacts, and accuracy of recovered intercellular stresses. PLoS One. 2013; 8:e55172. [PubMed: 23468843]

91. Lee EK, Kurokawa YK, Tu R, George SC, Khine M. Machine learning plus optical flow: a simple and sensitive method to detect cardioactive drugs. Sci Rep. 2015; 5:11817. [PubMed: 26139150]

92. Huebsch N, Loskill P, Mandegar MA, Marks NC, Sheehan AS, Ma Z, Mathur A, Nguyen TN, Yoo JC, Judge LM, Spencer CI, Chukka AC, Russell CR, So PL, Conklin BR, Healy KE. Automated Video-Based Analysis of Contractility and Calcium Flux in Human-Induced Pluripotent Stem Cell-Derived Cardiomyocytes Cultured over Different Spatial Scales. Tissue Eng Part C Methods. 2015; 21:467–479. [PubMed: 25333967]

93. Maddah M, Heidmann JD, Mandegar MA, Walker CD, Bolouki S, Conklin BR, Loewke KE. A non-invasive platform for functional characterization of stem-cell-derived cardiomyocytes with applications in cardiotoxicity testing. Stem Cell Reports. 2015; 4:621–631. [PubMed: 25801505]

94. Adrian, RJ.; Westerweel, J. Particle Image Velocimetry. Cambridge University Press, Place Published; 2001.

95. Priori SG, Napolitano C, Di Pasquale E, Condorelli G. Induced pluripotent stem cell-derived cardiomyocytes in studies of inherited arrhythmias. J Clin Invest. 2013; 123:84–91. [PubMed: 23281414]

96. Kim C, Wong J, Wen J, Wang S, Wang C, Spiering S, Kan NG, Forcales S, Puri PL, Leone TC, Marine JE, Calkins H, Kelly DP, Judge DP, Chen HS. Studying arrhythmogenic right ventricular dysplasia with patient-specific iPSCs. Nature. 2013; 494:105–110. [PubMed: 23354045]

97. Ma D, Wei H, Lu J, Ho S, Zhang G, Sun X, Oh Y, Tan SH, Ng ML, Shim W, Wong P, Liew R. Generation of patient-specific induced pluripotent stem cell-derived cardiomyocytes as a cellular model of arrhythmogenic right ventricular cardiomyopathy. Eur Heart J. 2013; 34:1122–1133. [PubMed: 22798562]

98. Rajamohan D, Matsa E, Kalra S, Crutchley J, Patel A, George V, Denning C. Current status of drug screening and disease modelling in human pluripotent stem cells. Bioessays. 2013; 35:281–298. [PubMed: 22886688]

99. Mercola M, Colas A, Willems E. Induced pluripotent stem cells in cardiovascular drug discovery. Circ Res. 2013; 112:534–548. [PubMed: 23371902]

100. Dell'Era P, Benzoni P, Crescini E, Valle M, Xia E, Consiglio A, Memo M. Cardiac disease modeling using induced pluripotent stem cell-derived human cardiomyocytes. World J Stem Cells. 2015; 7:329–342. [PubMed: 25815118]

101. Lopaschuk GD, Folmes CD, Stanley WC. Cardiac energy metabolism in obesity. Circ Res. 2007; 101:335–347. [PubMed: 17702980]

102. Peura JL, Scheffer JE. Lipotoxicity in the cardiac and skeletal muscle. Heart Metab. 2006; 30:4–6.

103. Heather LC, Clarke K. Metabolism, hypoxia and the diabetic heart. J Mol Cell Cardiol. 2011; 50:598–605. [PubMed: 21262230]
104. Zimmet P, Alberti KG, Shaw J. Global and societal implications of the diabetes epidemic. Nature. 2001; 414:782–787. [PubMed: 11742409]
105. Nakamura K, Hirano K, Wu SM. iPS cell modeling of cardiometabolic diseases. J Cardiovasc Transl Res. 2013; 6:46–53. [PubMed: 23070616]
106. Schweiger M, Lass A, Zimmermann R, Eichmann TO, Zechner R. Neutral lipid storage disease: genetic disorders caused by mutations in adipose triglyceride lipase/PNPLA2 or CGI-58/ABHD5. Am J Physiol Endocrinol Metab. 2009; 297:E289–296. [PubMed: 19401457]
107. Roden DM. Clinical practice. Long-QT syndrome. N Engl J Med. 2008; 358:169–176. [PubMed: 18184962]
108. Waring MJ, Arrowsmith J, Leach AR, Leeson PD, Mandrell S, Owen RM, Pairaudeau G, Pennie WD, Pickett SD, Wang J, Wallace O, Weir A. An analysis of the attrition of drug candidates from four major pharmaceutical companies. Nat Rev Drug Discov. 2015; 14:475–486. [PubMed: 26091267]
109. Mullard A. New drugs cost US[dollar]2.6 billion to develop. Nat Rev Drug Discov. 2014; 13:877–877.
110. Herper, M. The truly staggering cost of inventing new drugs, Forbes [online]. 2012. http://www.forbes.com/sites/matthewherper/2012/02/10/the-truly-staggering-cost-of-inventing-new-drugs/
111. Sager PT, Gintant G, Turner JR, Pettit S, Stockbridge N. Rechanneling the cardiac proarrhythmia safety paradigm: a meeting report from the Cardiac Safety Research Consortium. Am Heart J. 2014; 167:292–300. [PubMed: 24576511]
112. Lawrence CL, Pollard CE, Hammond TG, Valentin JP. Nonclinical proarrhythmia models: predicting Torsades de Pointes. J Pharmacol Toxicol Methods. 2005; 52:46–59. [PubMed: 15975832]
113. Kannankeril P, Roden DM, Darbar D. Drug-induced long QT syndrome. Pharmacological reviews. 2010; 62:760–781. [PubMed: 21079043]
114. Yang T, Snyders D, Roden DM. Drug block of I(kr): model systems and relevance to human arrhythmias. J Cardiovasc Pharmacol. 2001; 38:737–744. [PubMed: 11602820]
115. Aiba T, Shimizu W, Inagaki M, Noda T, Miyoshi S, Ding WG, Zankov DP, Toyoda F, Matsuura H, Horie M, Sunagawa K. Cellular and ionic mechanism for drug-induced long QT syndrome and effectiveness of verapamil. J Am Coll Cardiol. 2005; 45:300–307. [PubMed: 15653031]
116. Wu L, Shryock JC, Song Y, Belardinelli L. An increase in late sodium current potentiates the proarrhythmic activities of low-risk QT-prolonging drugs in female rabbit hearts. J Pharmacol Exp Ther. 2006; 316:718–726. [PubMed: 16234410]
117. Roden DM, Yang T. Protecting the heart against arrhythmias: potassium current physiology and repolarization reserve. Circulation. 2005; 112:1376–1378. [PubMed: 16145010]
118. May JE, Xu J, Morse HR, Avent ND, Donaldson C. Toxicity testing: the search for an in vitro alternative to animal testing. Br J Biomed Sci. 2009; 66:160–165. [PubMed: 19839229]
119. Price PS, Keenan RE, Swartout JC. Characterizing interspecies uncertainty using data from studies of anti-neoplastic agents in animals and humans. Toxicol Appl Pharmacol. 2008; 233:64–70. [PubMed: 18514247]
120. Sugiyama A. Sensitive and reliable proarrhythmia in vivo animal models for predicting drug-induced torsades de pointes in patients with remodelled hearts. Br J Pharmacol. 2008; 154:1528–1537. [PubMed: 18552873]
121. Townsend C, Brown BS. Predicting drug-induced QT prolongation and torsades de pointes: a review of preclinical endpoint measures. Curr Protoc Pharmacol. 2013 Chapter 10. Unit 10 16.
122. Qian JY, Guo L. Altered cytosolic Ca2+ dynamics in cultured Guinea pig cardiomyocytes as an in vitro model to identify potential cardiotoxicants. Toxicology in Vitro. 2010; 24:960–972. [PubMed: 20064605]
123. Wohlfart B. Analysis of mechanical alternans in rabbit papillary muscle. Acta Physiol Scand. 1982; 115:405–414. [PubMed: 6184949]

124. Verrier RL, Klingenheben T, Malik M, El-Sherif N, Exner DV, Hohnloser SH, Ikeda T, Martinez JP, Narayan SM, Nieminen T, Rosenbaum DS. Microvolt T-wave alternans physiological basis, methods of measurement, and clinical utility–consensus guideline by International Society for Holter and Noninvasive Electrocardiology. J Am Coll Cardiol. 2011; 58:1309–1324. [PubMed: 21920259]

125. Verrier RL, Malik M. Quantitative T-wave alternans analysis for guiding medical therapy: an underexploited opportunity. Trends Cardiovasc Med. 2015; 25:201–213. [PubMed: 25541329]

126. Kanaporis G, Blatter LA. The mechanisms of calcium cycling and action potential dynamics in cardiac alternans. Circ Res. 2015; 116:846–856. [PubMed: 25532796]

127. Sharma A, Burridge PW, McKeithan WL, Serrano R, Holmström A, Churko JM, Matsa E, Zhang Y, Kumar A, Álamo JCd, Mercola M, Wu SM, Wu JC. High-Throughput Screening of Tyrosine Kinase Inhibitors in Human Induced Pluripotent Stem Cell-Derived Cardiomyocytes Reveals a Class-Specific Cardiotoxicity Pattern, submitted. 2016

128. Chaudhari U, Nemade H, Wagh V, Gaspar JA, Ellis JK, Srinivasan SP, Spitkovski D, Nguemo F, Louisse J, Bremer S, Hescheler J, Keun HC, Hengstler JG, Sachinidis A. Identification of genomic biomarkers for anthracycline-induced cardiotoxicity in human iPSC-derived cardiomyocytes: an in vitro repeated exposure toxicity approach for safety assessment. Arch Toxicol. 2015

129. Ewer MS, Ewer SM. Cardiotoxicity of anticancer treatments. Nat Rev Cardiol. 2015; 12:620. [PubMed: 26292190]

130. Hahn VS, Lenihan DJ, Ky B. Cancer therapy-induced cardiotoxicity: basic mechanisms and potential cardioprotective therapies. J Am Heart Assoc. 2014; 3:e000665. [PubMed: 24755151]

131. Gaspar JA, Doss MX, Hengstler JG, Cadenas C, Hescheler J, Sachinidis A. Unique metabolic features of stem cells, cardiomyocytes, and their progenitors. Circ Res. 2014; 114:1346–1360. [PubMed: 24723659]

132. Liang P, Lan F, Lee AS, Gong T, Sanchez-Freire V, Wang Y, Diecke S, Sallam K, Knowles JW, Wang PJ, Nguyen PK, Bers DM, Robbins RC, Wu JC. Drug screening using a library of human induced pluripotent stem cell-derived cardiomyocytes reveals disease-specific patterns of cardiotoxicity. Circulation. 2013; 127:1677–1691. [PubMed: 23519760]

133. Hwang PM, Sykes BD. Targeting the sarcomere to correct muscle function. Nat Rev Drug Discov. 2015; 14:313–328. [PubMed: 25881969]

134. Mathur A, Loskill P, Shao K, Huebsch N, Hong S, Marcus SG, Marks N, Mandegar M, Conklin BR, Lee LP, Healy KE. Human iPSC-based cardiac microphysiological system for drug screening applications. Sci Rep. 2015; 5:8883. [PubMed: 25748532]

135. Reddy S, Bernstein D. Molecular Mechanisms of Right Ventricular Failure. Circulation. 2015; 132:1734–1742. [PubMed: 26527692]

136. Feinstein JA, Benson DW, Dubin AM, Cohen MS, Maxey DM, Mahle WT, Pahl E, Villafane J, Bhatt AB, Peng LF, Johnson BA, Marsden AL, Daniels CJ, Rudd NA, Caldarone CA, Mussatto KA, Morales DL, Ivy DD, Gaynor JW, Tweddell JS, Deal BJ, Furck AK, Rosenthal GL, Ohye RG, Ghanayem NS, Cheatham JP, Tworetzky W, Martin GR. Hypoplastic left heart syndrome: current considerations and expectations. J Am Coll Cardiol. 2012; 59:S1–42. [PubMed: 22192720]

HIGHLIGHTS

- High throughput physiological assays are at the forefront of new methods of drug discovery and safety pharmacology
- Combined with patient-specific iPSC-derived cardiomyocytes, this new technology offers unprecedented opportunities for personalized medicine
- This review discusses the challenges of faithfully reproducing human cardiomyocyte physiology and disease manifestions, and offers some solutions on the horizon that will advance the technology.

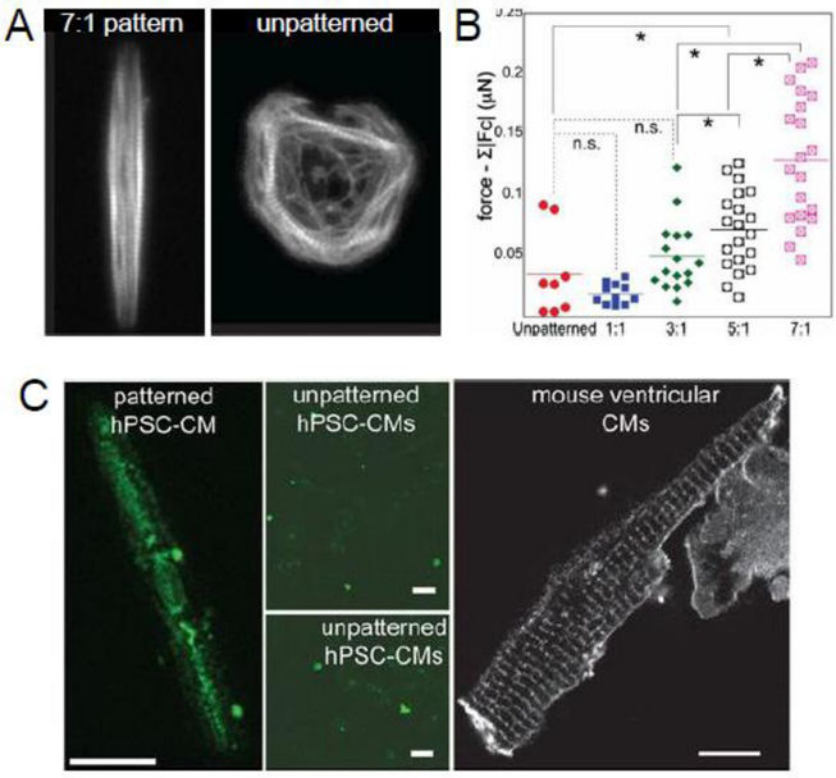

Figure 1. Matrigel micropatterns on traction-sensitive polyacrylamide hydrogel devices constrain hPSC-CMs to controllable shapes and engineer their mechanical output

A) Human iPSC-cardiomyocytes were cultured on micropatterns to induce aspect ratios of 1:1–7:1 and areas of 2,000 μm^2. Lifeact-labeled actin in myofibrils in live iPSC-cardiomyocytes show sarcomeric organization.

B) Myofibril alignment leads to higher contractile forces in single human iPSC-cardiomyocytes. Σ|Fc| of engineered hPSC-CMs increases with aspect ratio of the cardiomyocytes on the micropatterned surfaes.

C) iPSC-cardiomyocytes labeled with di-8-ANEPPS to reveal T-tubules. (*Left*) iPSC-cardiomyocyte (7:1) (Scale bar, 25 μm.). (*Center*) Unpatterned iPSC-cardiomyocyte on a 10-kPa hydrogel shown in both *Top* and *Bottom* (Scale bars, 50 μm.). (*Right*) Isolated adult mouse ventricular cardiomyocyte (Scale bar, 25 μm.).

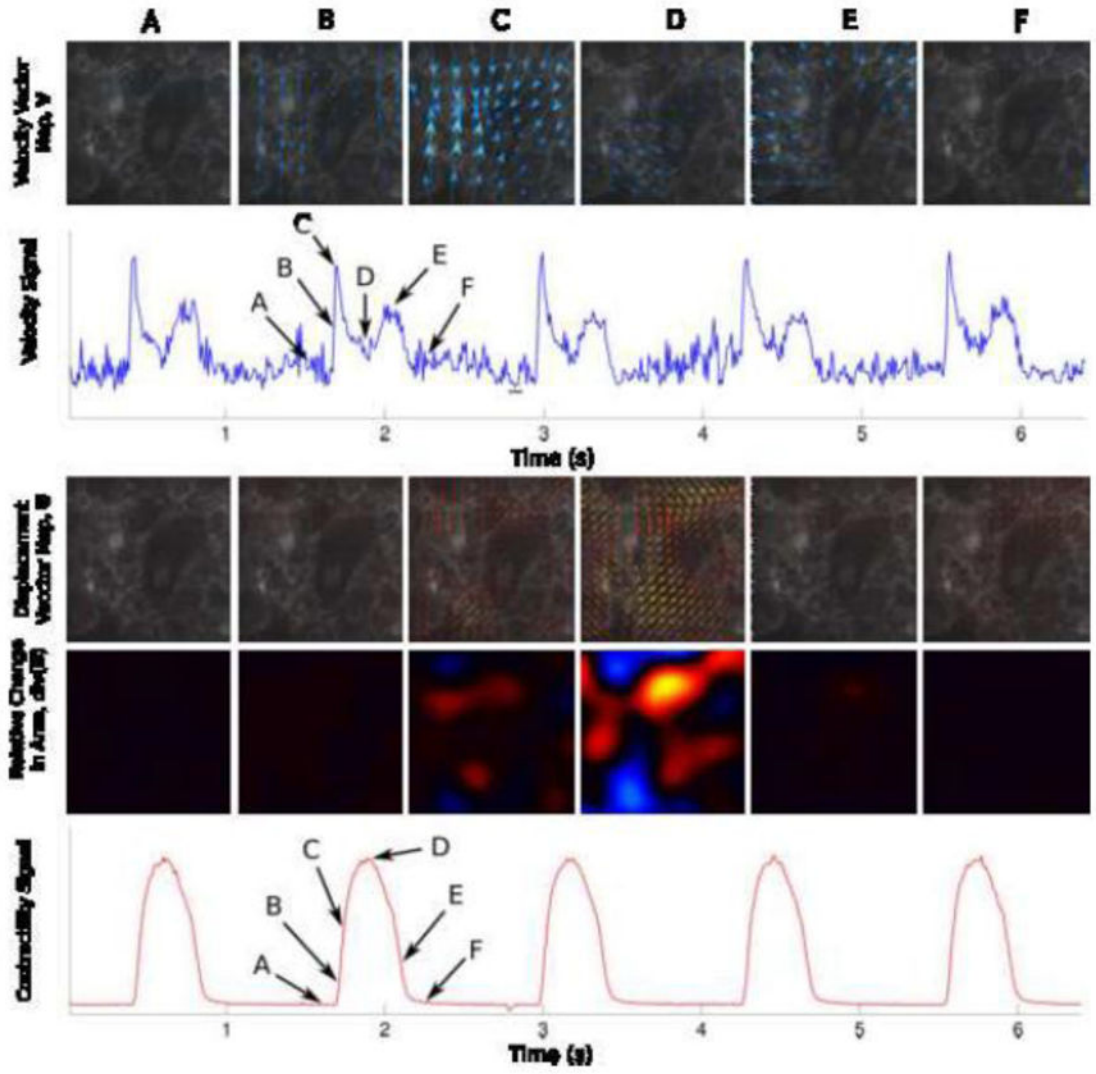

Figure 2. Measurement of iPSC-cardiomyocyte contractility from deformation maps

Top Row) Velocity maps shown at 6 different timeframes (A through F) corresponding to relevant events in the contraction cycle: Relaxed State, Beginning of the Contraction, Maximum Contraction Rate, Maximum Contraction, Maximum Relaxation Rate, and Relaxed State again.

Second Row) The Velocity Signal is obtained by taking the average of the magnitude of the each instantaneous velocity maps. The frame selection was done automatically. Selected reference frames (frames with least motion) are underlined in black.

Third Row) Displacement Vector Maps are computed using the individual timepoints relative to the reference frames. The 6 images represent the same maps (A through F) shown in the First Row.

Fourth Row) Within the displacement vector maps, the relative change in area (magnitude in color) is computed by direct application of Gauss' theorem.

Fifth Row) A contractility signal is obtained by taking the average of the magnitude of the relative change in area.

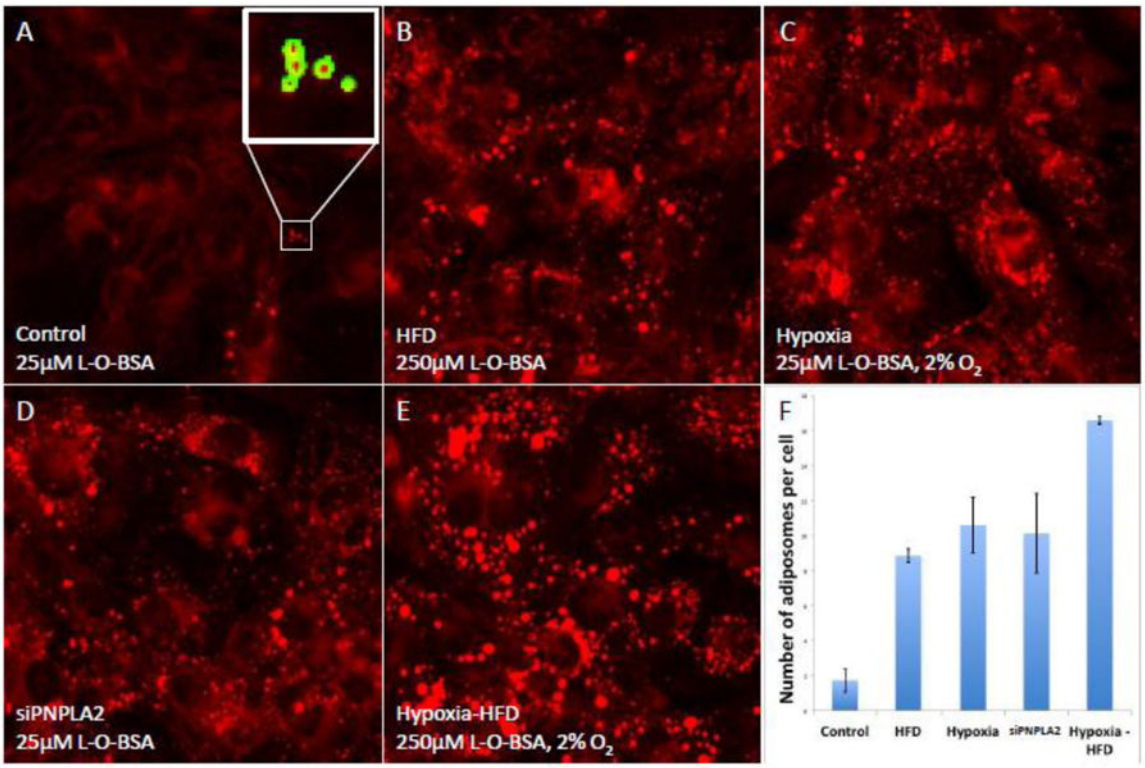

Figure 3. Modeling lipotoxicity in an iPSC-CM model

A) iPSC-CMs cultured in low fat media (supplemented with 25μM linoleic acid-oleic acid-albumin; L-O-BSA – Sigma, L9655) for one week have very few adiposomes.

B) Culturing iPSC-CMs with a "high fat diet" (HFD - 250μM L-O-BSA) results in increased number of adiposomes per cell.

C–E) This phenotype is recapitulated by culture in low fat media at hypoxia (2% O_2 for 48hrs) (C) or by siRNA-mediated PNPLA2 knockdown (D), and is exacerbated by the combination of hypoxia and HFD (E).

F) Quantification of the nile red-stained adiposomes (see A inset for example) using CellProfiler software

Table 1
Similarities and differences between Adult and iPSC-derived cardiomyocytes

Table modified from Knollmann [22]

iPSC-CM Features Similar to Human Adult CM	iPSC-CM Features Different From Human Adult CM
✓ Morphologically similar to Human Adult CMs	✓ iPSC-CM resemble immature human CMs
✓ All major types of ion channels present	✓ Relative expression of major ion channel types resemble neonatal and early postnatal CM profiles
✓ Contractile machinery present	✓ Diastolic membrane potential is −70/−60 mV
✓ Functional SR Ca stores present	✓ Spontaneously contracting cells
✓ Ca^{2+} handling is similar	✓ Low contractile force
✓ Ryanodine receptors present	✓ Lack of T-tubules and immature CICR
✓ Ca^{2+}-induced Ca^{2+} release present	✓ Large pacemaker currents (I_f) Small I_{K1}
✓ Atrial or ventricular-like APs are present	✓ Large IP3-sensitive Ca^{2+} stores
	✓ Variable cell size (cell capacitance ≈ from 30 to 150 pF)
	✓ β AR signaling is predominantly β1 AR; and signaling to PLN and cTn-I unrestricted

Table 2

Cardiomyocyte functional screening platforms

Throughput[1]	Recording Modality	System	Comments[2]	Recording Mode[3]
Low	Optical	Microscope	Very High Information content	Individual cells
Low	Electrophysiology	Manual Patch-Clamp	Very High Information content	Individual cells
Low	Planar Patch-Clamp	PatchXpress (Molecular Devices) Patchliner (Nanion Technologies GmbH) CytoPatch (Cytocentrics) SynchroPatch (Nanion Technologies GmbH)	Very High Information content	Individual cells
Low	Optical	ImageXpress Ultra Molecular Devices	Very High Information content	Individual cells
Low	Optical	ImageXpress® Micro Molecular Devices	High Information content	Individual cells
Medium	MEA	Maestro Axion Biosystems	Low Information content	Well/Multiple points
Medium	Impedance	xCELLigence ACEA Biosciences	Low Information content	Whole well
Medium	Planar Patch-Clamp	Sophion Qpatch and Sophion Qube (Biolin Scientific) CardioExcyte 96 (Nanion Technologies GmbH)	Medium Information content	Whole well
Medium	Planar Patch-Clamp	Axion MEA (Nanion Technologies GmbH)	Medium Information content	Well/Multiple points
Medium	Optical	Opera (Perkin Elmer)	High Information content	Individual cells
Medium	Optical	IC200 Kinetic Imaging Cytometer (Vala Sciences)	High Information content	Individual cells
High	Optical	FLIPR (Molecular Devices)	Low information content	Whole well
High	Optical	FDSS 7000 (Hamamatsu)	Low information content	Whole well

Notes:

[1]**Throughput:** Low, medium and high throughput estimates correspond to 1–2, up to 20, and 2000–20,000 compounds per day, respectively.

[2]**Information content:** Low, medium and high information content reflects the number of parameters that can be tested: 1, 2–4, >6 parameters per recording.

[3]**Recording mode** indicates that the platform records either whole well data, or individual cell data.